Article:

Griffin, J., Pearson, A.J., Scarratt, N.W. et al. (6 more authors) (2015) Organic photovoltaic devices with enhanced efficiency processed from non-halogenated binary solvent blends. Organic Electronics , 21. 216 - 222. ISSN 1566-1199

https://doi.org/10.1016/j.orgel.2015.03.019

Organic Photovoltaic Devices With Enhanced Efficiency Processed From Non-Halogenated Binary Solvent Blends

J. Griffin,[a] A. J. Pearson,[b] N.W. Scarratt,[a] T. Wang,[a] A.D.F. Dunbar,[c] H. Yi,[d] A. Iraqi,[d]
A.R. Buckley,[a] and D. G. Lidzey.[a]

[a] Department of Physics and Astronomy, University of Sheffield, Sheffield, S3 7RH, UK
[b] Optoelectronics Group, University of Cambridge, Cambridge, CB3 0HE, UK
[c] Department of Chemical and Biological Engineering, University of Sheffield, Sheffield, S1 3JD, UK
[d] Department of Chemistry, University of Sheffield, Sheffield, S3 7HF, UK

The development of processing routes to fabricate organic photovoltaic devices (OPVs) using non-halogenated solvents is a necessary step towards their eventual commercialisation. To address this issue, we have used Hansen solubility parameter analysis to identify a non-halogenated solvent blend based on a mixture of carbon disulfide and acetone. This solvent blend was then used to deposit a donor-acceptor polymer – fullerene thin-film that was then used as the active layer of bulk-heterojunction OPV. For the benchmark polymer:fullerene system PCDTBT:$PC_{70}BM$, a power conversion efficiency of 6.75% was achieved; a 20% relative improvement over reference cells processed using the chlorinated-solvent chlorobenzene. Improvements in device efficiency are attributed to an increase in electron and hole conductivity resulting from enhanced fullerene crystallisation; a property that leads to enhanced device efficiency through improved charge extraction.

1. Introduction

Bulk-heterojunction organic photovoltaic devices (BHJ OPVs) have seen rapid improvements in power conversion efficiency (PCE) over the past few years, resulting from improvements in the design of new semiconductors and the optimization of device architectures. Current record PCE's for single junction OPVs have seen dramatic leaps with the polymer PTB7 capable of exceeding 9% and most recently a PCE of 10.8% has been achieved using the polymer PffBT4T-2OD, these values are approaching the value deemed viable for commercial adoption.[1-4] We note however that most work on the development OPV devices has concentrated on the use of halogenated solvents (e.g. chlorobenzene) to solubilise and deposit the active semiconducting layer. Whilst such solvents enable uniform thin-films to be cast having a BHJ nanomorphology that is optimised for efficient photocurrent generation, environmental concerns place restrictions upon the use of halogenated solvents in an industrial environment; an issue that is problematic for the commercialization of high-performance OPVs.[1,5,6] Unfortunately, many organic semiconductors have poor solubility in non-halogenated solvents; a property that results in the formation of non-uniform thin-films that have poor photocurrent generating properties when fabricated into an OPV.

To address this, attention has focussed on the synthesis of high-performance organic semiconductors having improved solubility in non-halogenated solvents such as alcohols or water. Unfortunately the presence of additional solubilising side-groups can both increase the density of charge traps and result in the formation of a non-optimal active-layer morphology leading to a reduction in PCE.[7-10] An alternative approach is to use blends of non-halogenated solvents to mimic the solubility characteristics of a halogenated solvent. Here, the solubility of a material can be estimated by matching the Hansen solubility parameters (HSPs) of a blend of solvents to a specific solvent that is able to solubilise the desired material.[11] The HSP of a solvent consists of three components; the energy of the dispersion forces between molecules (δ_d), the energy resulting from permanent dipole moments (δ_p), and the energy of hydrogen bonds (δ_h). This powerful technique has been previously used to determine the solubility of a number of material systems including small molecule organic semiconductors.[12] HSP analysis has also been used to develop non-halogenated solvent blends to process a mixture of the polymer P3HT (poly(3-hexylthiophene-2,5-diyl)) and the fullerene acceptor $PC_{60}BM$ ([6,6]-phenyl-C_{61}-butyric acid methyl ester) with PV devices created having a PCE of up to 3.4%.[13-15] In other work, non-halogenated solvent systems have been developed to solubilise OPV active-layers based on the polymers PIDT-phanQ, PIDTT-DFBT, and PBDT-DTNT. Here, a solvent blend based on a mixture of the solvents toluene:1-methylnaphthalene and o-xylene:1,2-dimethylnaphthalene, with the devices created having a PCE of 6.1%, 7.2% and 6.1% respectively. It was however found that these systems required strict control over solvent blend composition to optimize device efficiency.[16,17]

Here, we report the use of a blend of carbon disulfide and acetone to cast the active semiconducting layer of an OPV consisting of a blend of the polymer PCDTBT ((poly[N-9'-heptadecanyl-2,7-carbazole-alt-5,5-(4',7'-di-2-thienyl-2',1',3'-benzothiadiazole)])) and $PC_{70}BM$ ([6,6]-Phenyl-C_{71}-butyric acid methyl ester). Average PCEs of 6.6% are achieved (peak 6.75%); a value that exceeds the efficiency achieved for reference devices cast from chlorobenzene (5.5%). In comparison to previous work on the use of HSP to develop non-halogenated solvent blends for OPV active layers [13], the replacement non-halogenated solvent blend we have developed here results in improved performance compared to its halogenated counterpart. Indeed, the PCEs values we have obtained using a non-halogenated solvent blend are close to the largest values that have been demonstrated for this donor:acceptor system using devices based on a ITO / Molybdenum (VI) Oxide anode and a Ca/Al cathode. We also show that this solvent system can be used to deposit a related polymer:fullerene system based on PFDT2BT-8 (poly[9,9-dioctylfluorene-4,7-alt-(5,6-bis(octyloxy)-4,7-di(2,2-bithiophene-5-yl)benzo[c]thiadiazole)-5,5-diyl]) and $PC_{70}BM$.[18] Here PCEs of 6.81% are achieved using the non-halogenated solvent blend compared to reference literature values of 5.8% achieved using chlorinated solvents. To understand such improvement in device performance, we apply a range of structural and optoelectronic probes to study the thin-films deposited including the use of grazing-incidence X-ray scattering to probe film structure at angstrom length scales. We demonstrate that films cast from non-halogenated solvents have improved electron- and hole-carrier conductivity that we speculate results from enhanced PCBM crystallisation; properties that are likely to reduce efficiency losses through geminate and non-geminate recombination.

2. Experimental

2.1 Materials

Carbon Disulfide (99.9% HPLC grade), acetone (99.5% HPLC grade) and chlorobenzene (99.95%) were purchased from Sigma Aldrich and used without any further purification. MoO_3 (99.95%) was purchased from Testbourne Ltd, vanadium (V) oxytriisopropoxide, Aluminium (99.99%) and Calcium (99%) were purchased from Sigma Aldrich. PCDTBT was synthesized according to previously reported methods,[19,20] and had a M_W of 26.5 KDa, and PDI of 2.18. PFDT2BT-8 was synthesized according to a previously reported method,[16] and had a M_W of 91.6 KDa, and PDI of 1.47. $PC_{70}BM$ was purchased from Ossila Ltd and had a purity of 95% (5% $PC_{60}BM$).

2.2 OPV fabrication and measurement

For PCDTBT:$PC_{70}BM$ devices ITO substrates were coated with a (8 nm) layer of Molybdenum (VI) Oxide for use as a hole extraction layer via vacuum evaporation. For PFDT2BT-8 devices vanadium (V) oxide was deposited via spin coating in air at speed of 4000 rpm from a precursor solution of vanadium (V) oxytriisopropoxide dissolved in isopropyl alcohol at a concentration of 4 mg ml^{-1}. The active layer was deposited from a solution of polymer:$PC_{70}BM$ dissolved in either chlorobenzene or a solvent blend of carbon disulfide and acetone (solvent blend ratio of 4:1) and with a polymer:fullerene blend ratio of 1:3.5 at an overall concentration of (25 mg ml^{-1} for PCDTBT devices and 35 mg ml^{-1} for PFDT2BT-8). Solutions were then spin coated at 4,300 RPM for CS_2:Acetone solutions and 1,800 RPM for chlorobenzene solutions. Devices were then transferred into a vacuum chamber for the deposition of the top calcium (3 nm) /aluminium (100 nm) cathode via vacuum evaporation in order to enhance hole blocking and reflectivity at the electron extracting interface.[21] Devices were encapsulated under nitrogen using a glass slide fixed in place by an inert UV-setting epoxy. For each solvent system explored, we have fabricated 4 independent devices-substrates, each containing 6 individual pixels (having an area of 4.8 mm^2) corresponding to a total of 24 devices per solvent-system. OPV devices were measured under ambient conditions using a Keithley 2400 source meter and a Newport 92251A-1000 AM1.5 solar simulator. A shadow mask was used to define the area of illumination as 4.5 mm^2. An NREL calibrated silicon diode was used to calibrate the power output at 100 $mWcm^{-2}$ at 40°C. In our data analysis, we have selected the top 50% of pixels having the highest efficiency from each deposition condition. This was done in order to remove any failed pixels and prevent any selection bias. EQE measurements were also recorded at Jsc for champion devices cast from the two different solvent blends.

2.3 Fabrication of Devices Having Conductivity Dominated by a Single Charge Carrier

Devices were fabricated in which charge conductivity is assumed to be dominated by electrons. Electron-dominated devices were based on a ITO/CS_2CO_3/PCDTBT:$PC_{70}BM$/Ca/Al architecture. J-V characteristics were measured in the dark over the voltage range 0 to 10 V. Data presented has been corrected for the built-in voltage of each device (estimated from the difference in electrode work functions) . A total of 31 devices (for CB) and 14 devices (for CS_2:Acetone) were fabricated to obtain average values.

2.4 GIWAXS

Wide-angle X-ray Diffraction patterns were obtained for each thin-film in a grazing-incidence geometry at the I07 beam-line at the Diamond Light Source (Didcot, UK). PCDTBT and PCDTBT:$PC_{70}BM$ blend films were deposited via spin-casting onto silicon/native oxide substrates for measurement. Samples were measured within a custom-built cell containing a slight overpressure of helium to minimise background X-ray scatter. For measurement, an 8 keV X-ray beam was incident on the sample surface at a grazing-incidence angle of 0.2°. Data was collected using a Pilatus 2M detector and analysed using the DAWN software package (http://www.dawnsci.org). Silver Behanate powder was used as a calibrant. Out-of-plane X-ray scattering profiles were obtained from a 20° wide sector-integration of the 2D GIWAXS images, whereas azimuthal X-ray scattering profiles were obtained over the q range 1 $Å^{-1}$ to 1.71 $Å^{-1}$ for PCDTBT:$PC_{70}BM$ films, and from 1.21 $Å^{-1}$ to 1.89 $Å^{-1}$ for PCDTBT films. Data plots were normalized to q_z values of 0.9 for the polymer:fullerene blend films and at $q_z = 2.3$ for the polymer films.

2.5 Photoluminescence Measurements

PL measurements were recorded using a 532 nm CW laser having a power of approximately 100 mW as an excitation source, with photoluminescence imaged into a monochromator coupled to silicon photodiode. All samples were held under vacuum during the course of the measurement.

3 Results

3.1 Identification of a Suitable Solvent Blend

The two prototypical donor-acceptor copolymers we have explored are shown in Figure 1 (a) and (b). Copolymer PFDT2BT-8 (shown in part (b)) has a similar structure to PFDTBT (poly[9,9-dioctyl-9H-fluorene-2,7-diyl-alt-(4,7-di-thiophen-2-yl)-2',1',3'-benzothiadiazole-5,5-diyl]) (shown in part (a)), but has two additional solubilising octyloxy groups on the benzothiadiazole unit and two extra thiophene units along the polymer backbone. Such modifications to the copolymer structure result in enhanced material solubility and a relative red-shift in the onset of optical absorption. Both PCDTBT and PFDT2BT-8 have relatively deep highest-occupied molecular orbital (HOMO) levels at approximately -5.3 eV relative to vacuum.

PCDTBT and PFDT2BT-8 are most often processed using chlorinated solvents such as chlorobenzene (CB). Chlorinated solvents such as CB pose many problems when it comes to the environmental damage they can cause. CB is, for example, highly toxic to aquatic life at very low concentrations and has a tendency to accumulate within water due to its low volatility, high-stability and solubility in water. To find a non-halogenated solvent replacement for CB, we have used Hansen solubility parameter analysis to obtain a solvent mixture having similar solubilizing properties as CB. This concept is illustrated in Figure 1(c) where we shown a three-dimensional plot of δ_p, δ_h and δ_d for CB, with Figure 1(d) plotting the same information on a Teas diagram. Clearly, there are a large number of ways by which solubility parameters can be matched. Here, we have chosen to use a combination of non-halogenated solvents that have similar values of δ_d to that of CB, but have values of δ_p and δ_h that are either relatively higher or lower than those of CB. On mixing, this combination of solvents permits a non-halogenated solvent system to be realised having very similar values of $\delta_{p,}$ δ_d and δ_h to that of CB.

The solvents we have chosen for this purpose are carbon disulfide (CS_2) and acetone. Acetone is a well-known solvent that is widely used in research and industry and has been applied in many commercial products including rayon and cellophane. CS_2 is used in the manufacture of rubber and was used as a precursor for carbon tetrachloride for most of the 20th century.[22,23] Compared to CB, CS_2 has lower impact in the environmental due to its relatively low toxicity, high-volatility and lower degree of solubility in water. CS_2 is also unstable upon exposure to sunlight and has a half-life in air of 5.5 days and 11 minutes in water. This combination of factors suggests it is less harmful to the environmentally than other chlorinated solvents. For completeness however, we emphasise that CS_2 is flammable due to its low boiling point, and it thus has an increased risk of ignition compared to other higher boiling-point organic solvents. Care should therefore be taken when handling large quantities of the solvent, however simple precautionary measures can be taken to reduce such risks.

CS_2 has HSP values of δ_p and δ_h that are lower than that of CB, with δ_p and δ_h of acetone both being significantly larger than that of CB as can be seen in Figures 1(c) and (d) and in **Table 1**. A further important consideration in our solvent selection is the fact that CS_2 and acetone are mutually miscible and have similar boiling points (46.0 and 56.1°C respectively). This latter property ensures that the solvents in the blend evaporate at a similar rate and that the Hansen solubility parameter of the blend does not change appreciably during the drying process. It should be noted however that both solvents have a boiling point that is significantly lower than that of chlorobenzene (131.7°C) and thus an CS_2:Acetone blend will dry more rapidly than CB.

In **Figure 1**(c) and (d) it can be seen that the best matching of HSPs to that of CB occurs when CS_2 and acetone are mixed at a composition of 83:17 by volume. We find that it is possible to dissolve PCDTBT, PFDT2BT-8, and $PC_{70}BM$ in CS_2:Acetone over a relatively larger range of blend ratios. Importantly, we find that at the optimal blend ratio, PCDTBT is slightly more soluble in the optimised

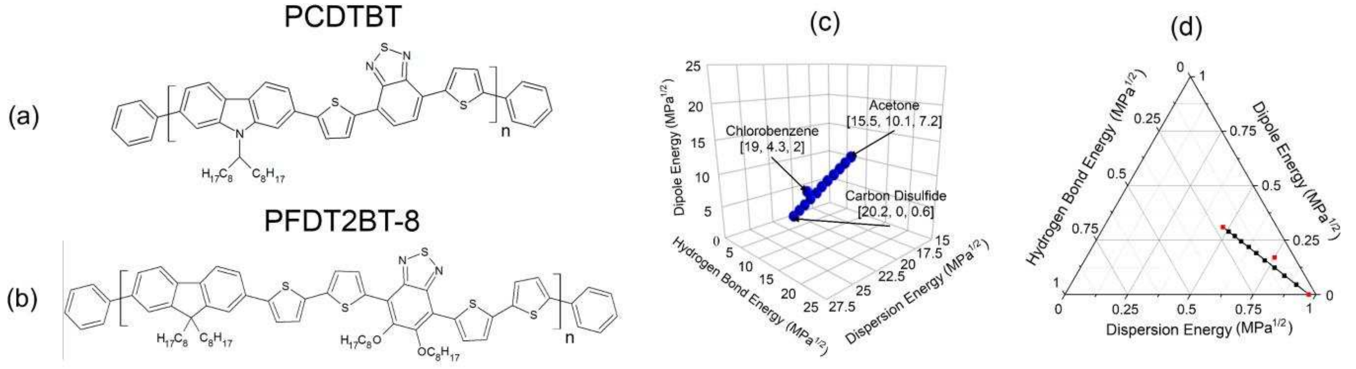

Figure 1. The chemical structure of the donor-acceptor copolymers PCDTBT and PFDT2BT-8 are shown in parts (a) and (b) respectively. Blends of carbon disulfide and acetone and their equivalent Hansen solubility parameters ranging from 9:1 to 1:9 by volume are plotted in a three dimensional plot (c) and a Teas diagram (d). In addition the locations of chlorobenzene, acetone and carbon disulfide are shown.

	δ_d (MPa)	δ_p (MPa)	δ_h (MPa)	Bpt (°C)	Visc. (mPa.s)*	Surf. Ten. (N.m^{-1})†
CS_2	20.2	0	0.6	46[25]	0.352[25]	0.0323[26]
C_3H_6O	15.5	10.1	7.0	56.1[25]	0.306[25]	0.0240[26]
C_6H_5Cl	19	4.3	2	131.7[25]	0.753[25]	0.0375[26]

* at 25°C, † at 20°C

Table 1. Hansen solubility parameters, boiling point, viscosity, and surface tension of the solvents carbon disulfide, acetone and chlorobenzene.

CS_2:Acetone blend than it is in CB, having a solubility limit of 20 mg ml^{-1} in the non-halogenated blend compared to 10 mg ml^{-1} for CB.

This apparent increase in the solubility of the PCDTBT in the CS_2:Acetone blend results from the fact that the Hansen solubility parameter of the solvent blend is a closer match to the ideal solvent characteristics for PCDTBT than is CB. This promising result indicates the suitability of this novel solvent blend for deposition techniques that require much higher concentration solutions.[24] Here, we determined the relative solubility of PCDTBT and $PC_{70}BM$ by dissolving in pure CS_2 at a concentration of 10 mg ml^{-1} and diluting with acetone to achieve specific %volumes of carbon disulfide. Images of solutions at varying %volumes of CS_2 are shown in supplementary data **Figure S1**. At 60% CS_2 and above, both materials are relatively soluble with few aggregates present in PCDTBT based solutions. Upon reducing the CS_2 concentration to 56% and below, it is observed that PCDTBT begins to come out of solution and forms small deposits on the side of the vials. $PC_{70}BM$ however remains in solution at much lower CS_2 concentrations.

3.2 OPV Device Results

We have fabricated OPV devices utilising an active layer of PCDTBT:$PC_{70}BM$ (1:3.5 wt%) that was deposited by spin-casting from either a CB or a CS_2:Acetone blend. **Figures 2(a)** and **(b)** show the J-V curves and external quantum efficiency (EQE) spectra for the highest performing devices fabricated from the two different casting solvents. Device metrics (peak and average PCE) are summarised in **Table 2**. Although the difference in J_{SC} determined for the different devices is the same within experimental uncertainty, we find that the current density at the maximum power point is significantly larger than experimental uncertainty level. Indeed, we find that devices cast from CS$_2$:Acetone exhibit an overall higher PCE compared to the CB reference cells with values of (6.6 ± 0.1)% and (5.5 ± 0.1)% determined for each sample set respectively. This 20% increase in PCE results from an increase in J$_{SC}$ (by 7.7%), FF (by 10%) and V$_{OC}$ (by 2.2%). From the EQE measurements presented in **Figure 2(b)**, it can be seen that the conversion efficiency of incident photons to extracted charge carriers is also higher for devices cast from a CS$_2$:Acetone blend compared to those cast from CB, taking a maximum EQE values of 75% and 68% respectively. Notably, the shape of the EQE spectrum of the CS$_2$:Acetone and CB prepared devices are slightly different, with the CS$_2$:Acetone device absorbing light more effectively between ~ 500 to 650 nm.

We have studied relative sensitivity of device performance to the solvent blend ratio, and have fabricated OPV devices in which the %volume of carbon disulfide added to the casting solvent was varied between 60% and 100%. Results are shown in supplementary data **Figure S2** in which we plot device J-V characteristics, with efficiency metrics summarised in **Table S1**. We find that for casting solvents containing between 60% and 90% CS$_2$ by volume, the PCE of solar cell devices is relatively constant, taking values between 6.3% and 6.5%. For devices prepared using pure CS$_2$, the PCE undergoes a strong reduction to around 2.5%; a result we as we discuss below results from charge extraction being compromised in these devices. This consistently high PCE across such a range of solvent composition is extremely promising, as many previous attempts at halogenated solvent replacement have reported narrower process windows.[12-17]

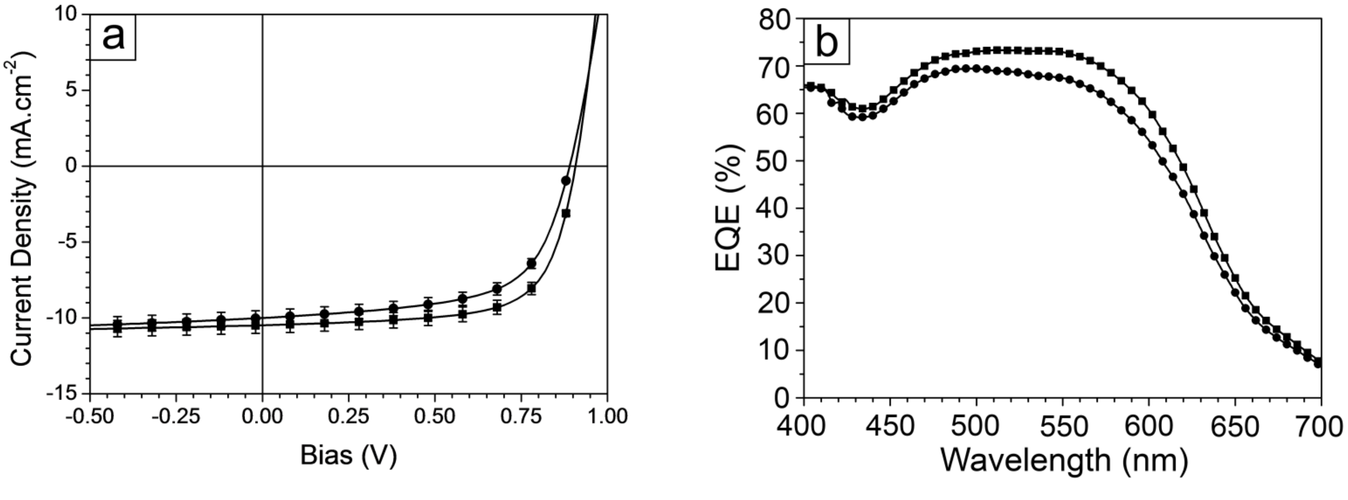

Figure 2. (a) J-V and (b) EQE graphs of peaks performing devices for (●) chlorobenzene devices and (■) carbon disulfide: acetone devices at an 8:2 solvent blend ratio.

Device (Solvent)	J_{sc} (mA.cm^{-2})	V_{oc} (V)	FF (%)	PCE (%)	R_S (Ω.cm^2)	R_{SH} (Ω.cm^2)
PCDTBT:PC$_{70}$BM (Chlorobenzene)	-10.00 (0.22) [-10.41]	0.89 (0.002) [0.89]	62.04 (1.01) [62.83]	5.52 (0.12) [5.80]	11.2 (1.6) [10.3]	829 (64) [730]
PCDTBT:PC$_{70}$BM (CS_2:Acetone)	-10.72 (0.16) [-10.72]	0.91 (0.002) [0.91]	68.20 (1.26) [69.40]	6.62 (0.13) [6.75]	7.1 (0.7) [6.9]	1669 (303) [1448]

Table 2. Device metrics showing average, (standard deviation), and [best device] values for the short circuit current density, open circuit voltage, fill factor, power conversion efficiency, series resistance, and shunt resistance for films cast from chlorobenzene or a carbon disulfide:acetone blend.

To explore the generality of this non-halogenated solvent system to deposit polymer-fullerene thin films having improved OPV efficiency, we have used it to process a blend of the polymer PFDT2BT-8 (see chemical structure in **Figure 1(b)**) and PC$_{70}$BM. We find that using the CS_2:Acetone solvent blend, devices had a maximum PCE = 6.81%, with V_{oc} = 0.94V, J_{sc} = -10.68 mA cm^{-2} and FF = 67.8% (see supplementary information **Figure S3** and **Table S2**). Again, we find that this power conversion efficiency is significantly higher than previously reported literature figures for this polymer:fullerene system in which a PCE of 5.8% was achieved when cast from chlorobenzene.[18]

3.3 Charge Carrier Conductivity

To identify the origin for the enhanced PCE of solar cells prepared using the non-halogenated solvent blend, devices whose injection is dominated by electrons were fabricated to characterise the effective conductivity of PCDTBT:PC$_{70}$BM thin films. Here, devices dominated by electron transport were based on CS_2CO_3 and Ca/Al electrodes. The result of this measurement is shown in **Figure 3** where we present the current density (under dark injection) sustained by such devices as a function of E, where E is the average electric field applied across the device. We find that for devices prepared using a

CS_2:Acetone blend, the average electron-mobility extracted from the space charge limited current regime is approximately (4.2 ± 0.3) x 10^{-4} cm^2 V s^{-1}. For films prepared from chlorobenzene, an electron mobility value of (1.6 ± 0.1) x 10^{-4} cm^2 V s^{-1} is instead determined. We believe that this modest increase in mobility is consistent with reduced non-geminate recombination, more efficient charge extraction and thus the observed increase in FF and J_{SC}.

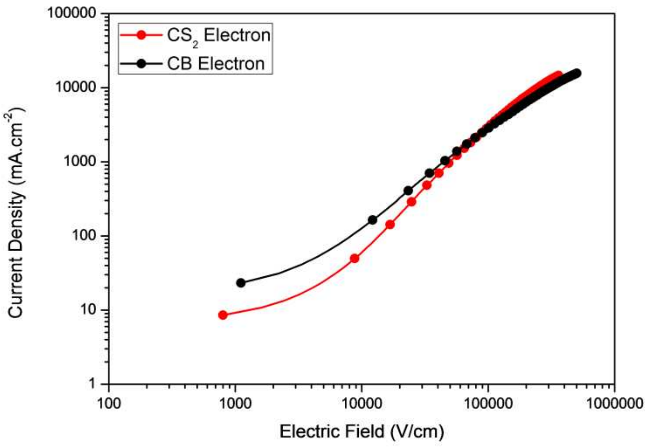

Figure 3. Current density as a function of the square root of electric field is shown for devices in which charge transport is dominated by electrons, cast from either chlorobenzene or a carbon disulphide-acetone blend.

3.4 Crystalline Structure of Deposited Films

To determine whether the different casting solvents modify the structure of the thin-film blend, we have used Grazing Incidence Wide Angle X-ray (GIWAXS) scattering to characterise the morphology of thin-films of PCDTBT and PCDTBT:PC_{70}BM. **Figure 4** shows scattering images for PCDTBT cast from (a) chlorobenzene and (b) CS_2:acetone, and a PCDTBT:PC_{70}BM blend cast from (c) chlorobenzene and (d) CS_2:acetone. Part (e), shows the intensity profile for each thin film as a function of q_z. Here the PCDTBT:PC_{70}BM scattering profiles have been displaced vertically for the sake of clarity.

Note, that the scattering background levels are similar in all samples studied. We are confident that the scattering patterns observed originate from molecular arrangement at nanometer length-scales, rather than diffraction effects from micron-sized PC_{70}BM clusters. We are confident that this is the case, as optical images of the films deposited are smooth and relatively uniform as can be seen in **Figure S4.**

Comparing the X-ray scattering pattern of pure PCDTBT cast from either CB or CS_2:Acetone (**Figure 4**(a) and (b) respectively), it can be seen that the polymer is largely amorphous when cast either both solvent system; a result in agreement with previous measurements.[27-29] Indeed, we confirm that X-ray scatter from the pure polymer is characterised by two broad rings located at approximately 0.42Å^{-1} (d-spacing of 15.0Å) and 1.61Å^{-1} (d-spacing of 0.39Å) in q_z that are attributed to lamellar packing and π-π stacking of adjacent polymer chains respectively.[27,29] Both rings are elliptical in nature with the regions of strongest X-ray scatter located in the out-of-place q_z direction. This indicates the existence of multiple polymorphs with a slight preference for face-on orientation of polymer chains with respect to the sample substrate. We find that the nature of the casting solvent does not affect the characteristic PCDTBT inter-chain spacing, however it appears that there is a relative increase in X-ray scattering intensity in the film cast from chlorobenzene, indicating enhanced crystallinity.

For the PCDTBT:$PC_{70}BM$ blend films (as shown in **Figure 4** parts (c) and (d)), we find that X-ray scatter is characterised by three distinct rings located in q_z at 0.67Å^{-1}, 1.38Å^{-1}, and 2.08Å^{-1}. These features derive from scattering from a hexagonal-close packed lattice of $PC_{70}BM$ aggregates within the blend and correspond to d-spacings of 0.94 nm, 0.46 nm and 0.30 nm respectively.[27,30] In **Figure 4**(e) it can be seen that there is a significant relative increase in scattering intensity from the $PC_{70}BM$ aggregates in the blend films cast from CS_2:Acetone (although the linewidth of this feature remains unchanged). We interpret this behaviour as originating from an increase in the number-density of fullerene aggregates within the CS_2:Acetone cast sample, rather than from differences in the size of the aggregates (a change in size would be evidenced by a change in scattering-feature linewidth). Such effects are not simply limited to PCDTBT-based blends. Indeed, increased scattering intensity associated with aggregated $PC_{70}BM$ is also observed in films of PFDT2BT-8:$PC_{70}BM$ cast from a CS_2:Acetone solvent blend (see **Figure S5**). This indicates that such effects are not just limited to a single polymer:fullerene system but may be more general over a large class of materials.

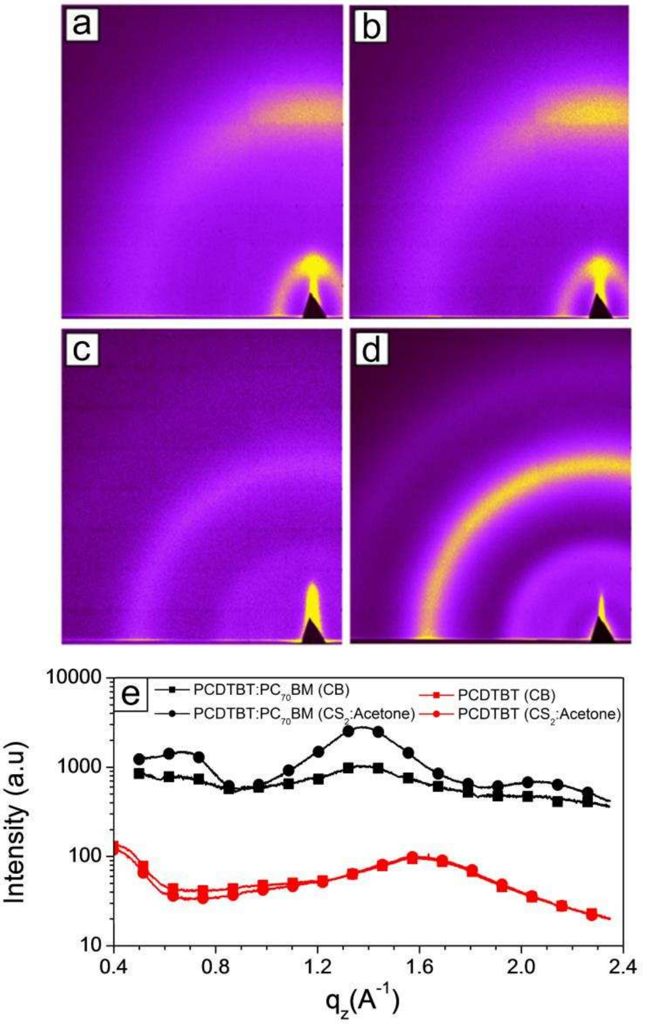

Figure 4. GIWAXS data showing scattering patterns for PCDTBT films cast from (a) chlorobenzene and (b) carbon disulfide: acetone blends. Parts (c) and (d) show scattering patterns for PCDTBT:$PC_{70}BM$ films cast from chlorobenzene and carbon disulfide respectively. In part (e) we plot scattering intensity along the q_z axis extracted from data presented in parts (a) to (d).

We can confirm this increase in aggregate number-density using steady-state photoluminescence (PL) measurements recorded from the CB and CS_2:Acetone solvent blend films as shown in **Figure 5**. Here, no normalisation is applied to these spectra, with the data presented being recorded under identical excitation conditions. For comparison, we also show PL emission recorded from a control film of pure $PC_{70}BM$. It can be seen that the emission from the PCDTBT:$PC_{70}BM$ films is almost identical to that of $PC_{70}BM$. Such luminescence from polymer:fullerene blends has been previously ascribed to radiative decay of excitons photo-generated on fullerene aggregates whose size is comparable to the diffusion length of a $PC_{70}BM$ exciton (~5nm);[31] a property that results in some fraction of excitons undergoing radiative recombination rather than dissociation into charge-carriers. It can be seen that the PL emission intensity associated with aggregated $PC_{70}BM$ is significantly greater (approximately 5 times) from films cast from a CS_2:Acetone solvent than it is for CB cast films. This observation further suggests that there is a relative increase in the fraction of $PC_{70}BM$ molecules that undergo aggregation within a CS_2:Acetone cast film.

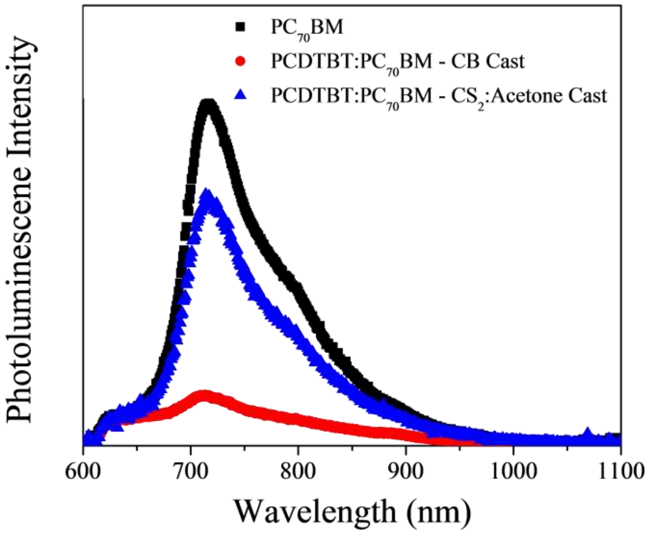

Figure 5. Steady state photoluminescence recorded from a PCBM film cast from CB, together with PL emission from PCDTBT:$PC_{70}BM$ blend films (1:3.5 wt%) cast from CB and a CS_2:Acetone solvent blend.

4. Conclusion

We believe that the enhanced $PC_{70}BM$ aggregation in thin-films cast from the solvent blend results from the greater relative solubility of $PC_{70}BM$ in a CS_2:Acetone solution even at relatively low CS_2 concentrations. We speculate that as the solvent-blend film evaporates, the relative concentration of CS_2 in the CS_2:Acetone blend falls due to its slightly greater volatility compared to acetone. When the CS_2 concentration falls below ~ 56%, the PCDTBT component starts to drop out of solution as its solubility limit has been reached. At this point however, the $PC_{70}BM$ still remains in solution and only forms aggregates at a later point in the evaporation process. This relative delay in the solidification between $PC_{70}BM$ compared to PCDTBT results in a film that has reduced mixing between the polymer and the fullerene, with a greater fraction of $PC_{70}BM$ being found in an aggregated form. Clearly, the difference in the volatility between CS_2 and acetone is sufficiently small to create a film in which there is still an effective dispersion of $PC_{70}BM$ molecules within a PCDTBT-rich matrix, rather than a system in which the two components are completely de-mixed.

We thus ascribe the improved electron mobility, FF and device efficiency on casting from a CS_2:Acetone blend to the increased aggregation and crystallization of the $PC_{70}BM$. It is possible that this improves device efficiency in several ways; firstly, a number of studies have argued that geminate- and non-geminate recombination is suppressed when an electron is created upon a $PC_{70}BM$ aggregate, rather than on an isolated molecule.[33,34] Secondly, the formation of a larger population of $PC_{70}BM$ aggregates will facilitate charge-extraction through the formation of percolation pathways.

We have shown therefore that a CS_2:Acetone blend can be used to form a solvent system able to effectively solubilize a number of prototypical organic semiconductors with such properties being maintained over a wide range of blend ratios. X-ray scattering measurements of films cast from the solvent blend demonstrate a significant increase in the fraction of fullerene molecules undergoing aggregation. This increased aggregation is beneficial for device performance, as it increases the efficiency of charge carrier extraction as evidenced by increased electron and hole conductivity and by improved device fill-factors. This permits us to realise PCDTBT:$PC_{70}BM$ OPVs having a maximum PCE of 6.75%, with similar devices based on PFDT2BT-8 having a PCE of 6.81%; values both larger than those realised in comparable devices in which the active layer was cast from a chlorinated solvent (chlorobenzene). Our results demonstrate therefore a simple and straight-forward approach to fabricate OPVs using solvents that are less harmful to the environment than regular chlorinated solvents. Critically, this selection of solvents does not sacrifice device performance, but leads to enhanced device efficiency.

Acknowledgements

We thank Richard T. Grant for help with photoluminescence measurements. We also thank the UK EPSRC for funding the project ‘Polymer fullerene photovoltaic devices: New materials and innovative processes for high-volume manufacture’ (EP/I02864/1) and ‘Supersolar Solar Energy Hub’ (EP/J017361/1). AJP thanks King Abdulaziz University for financial support via grant no. D-004/431.

[1] Z. He, C. Zhong, S. Su, M. Xu, H. Wu, Y. Cao, Nature Photon **2012**, 6, 591-595

[2] J. R. Sheats, J. Matter. Res. **2004**, 19, 1974-1989

[3] C. J. Brabec, Sol. Energy. Mater. Sol. Cells, **2004**, 83, 273-292

[4] Y. Liu, J. Zhao, Z. Li, C. Mu, W. Ma, H. Hu, K. Jiang, H. Lin, H. Ade, H. Yan, Nat. Commun. **2014**, 5, 5293

[5] G. Li, V. Shrotriya, J. Huang, Y. Yao, T. Moriarty, K. Emery, Y. Yang, Nature Mater. **2005**, 4, 864-868

[6] S. H. Park, A. Roy, S. Beaupré, S. Cho, N. Coates, J. S. Moon, D. Moses, M. Leclerc, K. Lee, A. J. Heeger. Nature, **2009**, 3, 297-302

[7] R. Søndergaard, M. Helgesen, M. Jørgensen, F. C. Krebs, Adv. Energy Mater. **2011**, 1, 68-71

[8] C. Duan, W. Cai, B. B. Y. Hsu, C. Zhong, K. Zhang, C. Liu, Z. Hu, F. Huang, G. C. Bazan, A. J. Heeger, Y. Cao, Energy Environ. Sci. **2013**, 6, 3022-3034

[9] J. K. Mwaura, M. R. Pinto, D. Witker, N. Ananthakrishnan, K. S. Schanze, J. R. Reynolds. Langmuir, **2005**, 21, 10119-10126

[10] T. R. Andersen, T. T. Larsen-Olsen, B. Andreasen, A. P. L. Böttiger, J. E. Carlé, M. Helgesen, E. Bundgaard, K. Norrman, J. W. Andreasen, M. Jørgensen, F. C. Krebs, ACS Nano, **2011**, 5, 4188-4196

[11] C. M. Hansen, A. L. Smith, Carbon **2004**, 42, 1591-1597

[12] I. Burgues-Ceballos, F. Machui, J. Min, T. Ameri, M. M. Voigt, Y. N. Luponosovo, S. A. Ponomarenko, P. D. Lachmaroise, M. Campoy-Quiles, C. J. Brabec. Adv. Funct. Mater. **2014**, 24, 1449-1457

[13] C. D. Park, T. A. Fleetham, J. Li, B. D. Vogt, Org. Electron. **2011**, 12, 1465-1470

[14] B. Schmidt-Hansberg, M. Sanyal, N. Grossiord, Y. Galagan, M. Baunach, M. F. G. Klein, A. Colsmann, P. Scharfer, U. Lemmer, H. Dosch, J. Michels, E. Barrena, W. Schabel, Sol. Energy Mater. Sol. Cells, **2012**, 96, 195-201

[15] F. Machui, S. Langner, X. Zhu, S. Abbott, C. J. Brabec. Sol. Energy Mater. Sol. Cells, **2012**, 100, 138-146

[16] K. S. Chen, H. L. Yip, C. W. Schlenker, D. S. Ginger, A. K. Y. Jen, Org. Electron. **2012**, 13, 2870-2878

[17] C. C. Chueh, K. Yao, H. L. Yip, C. Y. Chang, Y. X. Xu, K. S. Chen, C. Z. Li, P. Liu, F. Huang, Y. Chen, W. C. Chen, A. K. Y. Jen. Energy Environ. Sci. **2013**, 6, 3241-3248

[18] D. C. Watters, H. Yi, A. J. Pearson, J. Kingsley, A. Iraqi, D. G. Lidzey, Macromol. Rapid Commun. **2013**, 34, 1157-1162

[19] A. A. B. Alghamdi, D. C. Watters, H. Yi, S. Al-Faifi, M. S. Almeataq, D. Coles, J. Kingsley, D. G. Lidzey, A. Iraqi, J. Mater. Chem. A, **2013**, 1, 5165-5171

[20] N. Blouin, A. Michaud, M. Leclerc, Adv. Mater. **2007**, 19, 2295-2300

[21] D. C. Watters, J. Kingsley, H. Yi, T. Wang, A. Iraqi, D. G. Lidzey, Org. Electron. **2012**, 13, 1401-1408

[22] Agency for Toxic Substances and Disease Registry (ATSDR). 1996. Toxicological profile for Carbon Disulfide. Atlanta, GA: U.S. Department of Health and Human Services, Public Health Service.

[23] U.S. Environmental Protection Agency. Health and Environmental Effects Profile for Carbon disulfide. EPA/600/x-86/155. Environmental Criteria and Assessment Office, Office of Health and Environmental Assessment, Office of Research and Development, Cincinnati, OH. 1986

[24] F. C. Krebs, Sol. Energy Mater. Sol. Cells, **2009**, 93, 394-412

[25] D. R. Lide, Handbook of Chemistry and Physics. CRC Press, Boca Raton, United States **1998**

[26] J. A. Dean, *Lange's Handbook of Chemistry*, McGraw-Hill New York, United States **1999**

[27] P. A. Staniec, A. J. Parnell, A. D. F. Dunbar, H. Yi, A. J. Pearson, T. Wang, P. E. Hopkinson, C. Kinane, R. M. Dalgliesh, A. M. Donald, A. J. Ryan, A. Iraqi, R. A. L. Jones, D. G. Lidzey. Adv. Energy Mater. **2011**, 1, 499-504

[28] R. B. Aïch, N. Blouin, A. Bouchard, M. Leclerc, Chem. Mater. **2009**, 21, 751-757

[29] N. Blouin, A. Michaud, D. Gendron, S. Wakim, E. Blair, R. Neagu-Plesu, M. Belletête, G. Durocher, Y. Tao, M. Leclerc, J. Am. Chem Soc. **2008**, 130, 732-742

[30] T. Ohno, S. Yatsuya, J. Mater. Sci. **1998**, 33, 5843-5847

[31] S. D. Dimitrov, C. B. Nielsen, S. Shoaee, P. S. Tuladhar, J. Du, I. McCulloch, J. R. Durrant, J. Phys. Chem. Lett. **2012**, 3, 140-144

[32] K. Tvingstedt, K. Vandewal, F. Zang, O. Inganäs. J. Phys. Chem. C **2010**, 114, 21824-21832

[33] F. C. Jamieson, E. B. Domingo, T. McCarthy-Ward, M. Heeney, N. Stingelin, J. R. Durrant. Chem. Sci. **2012**, 3, 485-492

[34] S. Gélinas, A. Rao, A. Kumar, S. L. Smtih, A. W. Chin, J. Clark, T. S. Van der Poll, G. C. Bazan, R. H. Friend. Science, **2014**, 343, 512-516

Supplementary Information

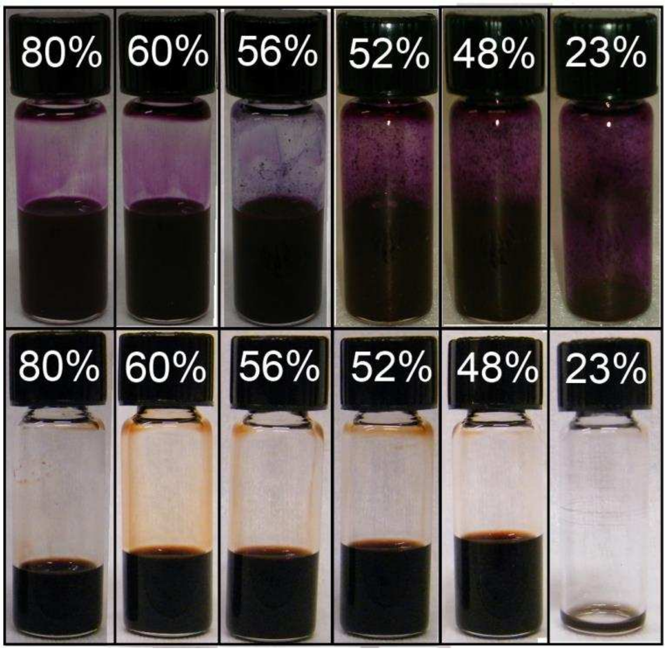

Figure S1. Images showing the relative solubility for PCDTBT (Top) and $PC_{70}BM$ (bottom) in blends of CS_2:Acetone with %volume of CS_2 shown, 23% volume has solvent removed from vial to show the amount of aggregates left upon the vial.

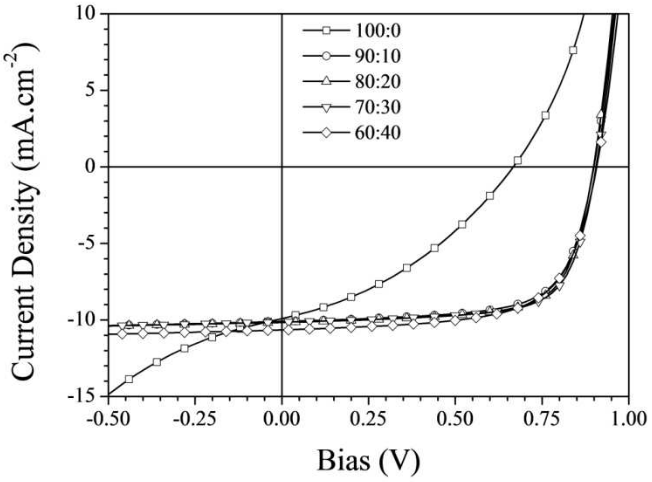

Figure S2. Average J-V characteristics of OPV devices cast from blends of CS_2:acetone, with the CS_2 concentration varied between 60 and 100 by volume.

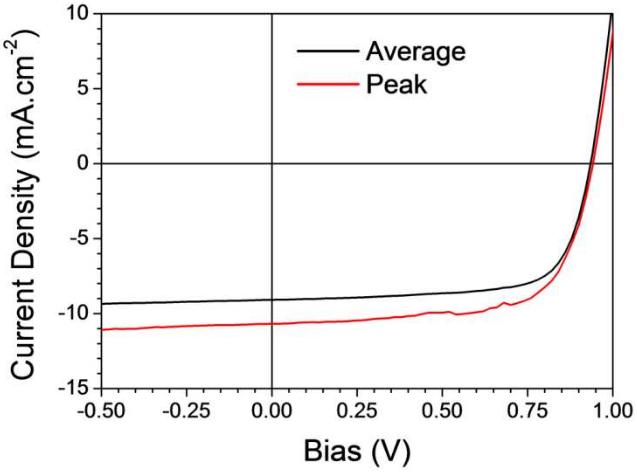

Figure S3. Average J-V characteristics of PFDT2BT-8:$PC_{70}BM$ OPV devices cast from a CS_2:acetone blend

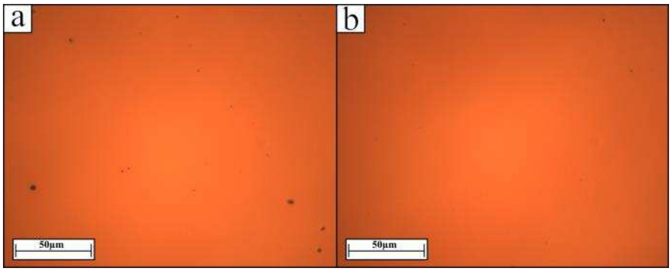

Figure S4. Optical microscopy images of films of PCDTBT:$PC_{70}BM$ cast from (a) Chlorobenzene and (b) CS_2:Acetone

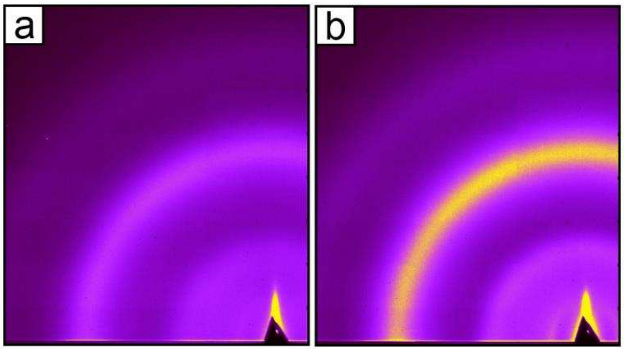

Figure S5. QIWAXS images of blends of PFDT2BT-8:$PC_{70}BM$ films cast from (a) CB and (b) CS_2:Acetone

Solvent Ratios (CS_2:Acetone)	J_{sc} ($mA.cm^{-2}$)	V_{oc} (V)	FF (%)	PCE (%)	R_S ($\Omega.cm^{-2}$)	R_{SH} ($\Omega.cm^{-2}$)
60:40	-10.66 (0.32) [-11.00]	0.91 (0.002) [0.91]	65.8 (2.1) [66.1]	6.36 (0.12) [6.57]	8.0 (0.5) [7.8]	1593 (173) [1230]
70:30	-10.12 (0.16) [-10.32]	0.91 (0.01) [0.91]	70.8 (5.0) [70.9]	6.51 (0.09) [6.64]	6.9 (0.1) [7.2]	2190 (373) [2361]
80:20	-10.16 (0.21) [-10.27]	0.90 (0.01) [0.90]	70.5 (1.2) [71.5]	6.43 (0.18) [6.61]	7.6 (0.3) [6.8]	1793 (418) [2028]
90:10	-10.09 (0.27)	0.90 (0.02)	69.3 (3.3)	6.29 (0.33)	7.8 (0.5)	1894 (423)

	[-10.18]	[0.91]	[71.5]	[6.60]	[7.1]	[1567]
100:0	-9.92 (0.25) [-10.11]	0.67 (0.06) [0.77]	37.0 (3.0) [45.7]	2.46 (0.45) [3.53]	32.6 (4.9) [13.8]	190 (56) [426]

Table S1. Device metrics showing average, (standard deviation), and [best device] values for the short circuit current density, open circuit voltage, fill factor, power conversion efficiency, series resistance, and shunt resistance for films cast from varying carbon disulfide: acetone blends.

	J_{sc} (mA.cm^{-2})	V_{oc} (V)	FF (%)	PCE (%)
PFDT2BT-8:$PC_{70}BM$	-9.08 (-10.68)	0.93 (0.94)	71.4 (67.8)	6.05 (6.81)

Table S2 Device metrics showing average, and (best device) values for the short circuit current density, open circuit voltage, fill factor, power conversion efficiency, series resistance, and shunt resistance for PFDT2BT-8:$PC_{70}BM$ devices cast from a CS_2:Acetone blend.